Sedimentary Geology 305 (2014) 69–82

Contents lists available at ScienceDirect

Sedimentary Geology

journal homepage: www.elsevier.com/locate/sedgeo

Pliocene mass failure deposits mistaken as submarine tsunami backwash sediments — An example from Hornitos, northern Chile

Michaela Spiske [a,*], Heinrich Bahlburg [a], Robert Weiss [b]

[a] Westfälische Wilhelms-Universität, Institut für Geologie und Paläontologie, Corrensstrasse 24, 48149 Münster, Germany
[b] Department of Geosciences, Virginia Tech, 4044 Derring Hall, Blacksburg, VA 24061, USA

ARTICLE INFO

Article history:
Received 19 December 2013
Received in revised form 18 March 2014
Accepted 19 March 2014
Available online 27 March 2014

Editor: J. Knight

Keywords:
Marine tsunami deposit
Backwash
Mass wasting
Debris flow
Mio-Pliocene
Eltanin impact

ABSTRACT

In this study we question the former interpretation of a shallow marine backwash tsunami origin of a conspicuous Pliocene coarse clastic unit at Hornitos, northern Chile, and instead argue for a debris flow origin for this unit. We exclude a relation to a tsunami in general and to the Eltanin impact in particular. The observed deposit at Hornitos was not generated either directly (impact-triggered tsunami) or indirectly (submarine mass flow caused by seismic shaking) by an impact. Re-calculation of the alleged impact tsunami including consideration of the Van Dorn effect shows that an impact in the Southern Ocean did not cause a significant tsunami at Hornitos. Impact-related seismic shaking was not able to trigger slides several thousands of kilometers away because the Eltanin event was a deep sea-impact that did not create a crater. Additionally, the biostratigraphic age of 5.1–2.8 Ma of the associated La Portada Formation is not concurrent with the newly established age of 2.511 ± 0.07 Ma for the Eltanin impact.

Instead, we argue for an origin of the conspicuous unit at Hornitos as a debris flow deposit caused by an earthquake in the Andean subduction zone in northern Chile. Our re-interpretation considers the local synsedimentary tectonic background, a comparison to recent submarine tsunami sediments, and recent examples of mass wasting deposits along the Chilean margin. The increased uplift during the Pliocene caused oversteepening of the coastal scarp and entailed a contemporaneous higher frequency of seismic events that triggered slope failures and cliff collapses. The coarse clastic unit at Hornitos represents an extraordinary, potentially tsunami-generating mass wasting event that is intercalated with mass wasting deposits on a smaller scale.

1. Introduction

Characteristic features of onshore tsunami deposits have been extensively studied over recent decades, especially during post-event surveys (e.g., Liu et al., 2005; Richmond et al., 2006; Bahlburg and Weiss, 2007; Bahlburg and Spiske, 2012; Goto et al., 2012; Richmond et al., 2012). While the characteristics of onshore deposits are well documented, the associated marine tsunami effects, such as sediment dispersion, erosion or deposition during run-up, and sediment bypassing, erosion or deposition caused by the backwash are scarcely known. So far, only a few studies document the impacts of recent tsunamis in marine environments. Marine disturbances and related erosion and sedimentation caused by the 2003 Tokachi-Oki tsunami were documented by Noda et al. (2007), those connected to the 2004 Indian Ocean tsunami by Di Geronimo et al. (2009), Feldens et al. (2009, 2012) and Paris et al. (2010), and the 2011 Tohoku tsunami by Kawagucci et al. (2012) and Arai et al. (2013).

A good understanding of the factors controlling the generation of both onshore and marine tsunami deposits is paramount for two reasons. Firstly, tsunami deposits often record the processes that form them (Huntington et al., 2007; Switzer et al., 2012). Second, marine sediments tend to be preferentially preserved in the pre-Quaternary geological record in comparison to coastal tsunami deposits that have a relatively low preservation potential (Spiske et al., 2013). This implies that studies of recent onshore tsunami deposits cannot necessarily be used as templates for the recognition of ancient tsunami sediments. There are several examples of unusual Precambrian to Pliocene submarine beds that have been attributed to the effects of a tsunami rather than to storms or mass wasting processes (e.g., Bailey and Weir, 1932; Ballance et al., 1981; Michalík, 1997; Hassler et al., 2000; Rossetti et al., 2000; Pratt, 2001, 2002; Scasso et al., 2005; Schnyder et al., 2005; Brookfield et al., 2006; Goto et al., 2008; Sarkar et al., 2011; Tachibana, 2013).

Recent review articles (e.g., Dawson and Stewart, 2008; Shiki et al., 2008; Sugawara et al., 2008; Bourgeois, 2009; Shanmugam, 2012) describe the characteristics of marine tsunami sediments. Erosional scours belong to these characteristics along with rip-up clasts, soft-sediment deformation, sand injections, parallel lamination, successions of sub-

* Corresponding author.
E-mail address: spiske@uni-muenster.de (M. Spiske).

http://dx.doi.org/10.1016/j.sedgeo.2014.03.003
0037-0738/

units each depicting normal grading and reflecting individual waves of the wave train, and indicators of opposite flow direction by run-up and backwash oscillations (e.g., ripples, antidunes, imbrication). Further features may be a mixture of faunal remains from different habitats, plant material indicating the terrestrial and therefore backwash origin of at least parts of the succession, and a chaotic mixture of boulders and clasts within a fine-grained matrix. Deposits generated by earthquake-triggered tsunamis may be underlain by sediments that display liquefaction, water escape structures, as well as fissures and clastic dykes caused by the seismic events. Impact-tsunami deposits may contain spherules or shocked quartz. However, the distinction of marine tsunami deposits and common turbidites may not always be possible, especially for fine-grained and distal (deep water) sediments. Furthermore, in shallow marine environments, tsunami sediments need to be discriminated from storm and flood deposits. Bourgeois (2009) notes that some of the literature describing ancient tsunami deposits is quite speculative and their interpretations may be wrong. The speculative origin of some of these sequences is underlined by several publications that re-interpret deposits which have previously been attributed to tsunami as the result of submarine debris flows or storm surges (e.g., Murty, 1982; Pickering, 1984; Bahlburg et al., 2010).

In Chile, a number of conspicuous sediment sequences found in formations of Miocene to Pliocene age have been interpreted as submarine tsunami backwash deposits (e.g., Le Roux et al., 2004; Cantalamessa and Di Celma, 2005; Le Roux and Vargas, 2005; Le Roux et al., 2008). One example is the Huentequapi sandstone as part of the Pliocene Ranquil Formation which is, like parts of the La Portada Formation, supposed to be related to the Eltanin impact (Le Roux et al., 2008; Goff et al., 2012). In contrast, broadly coeval deposits of very similar appearance at other locations and in similar tectonic environments were interpreted as submarine mass wasting deposits related to sea level changes and regional tectonics (e.g., Le Roux and Elgueta, 2000; Le Roux and Vargas, 2005; Le Roux et al., 2006). However, unequivocal evidence was not presented for any of the examples. In the case of the proposed Miocene submarine tsunami backwash deposits described by Cantalamessa and Di Celma (2005) at the Mejillones Peninsula, Bahlburg et al. (2010) argue that these deposits were the result of debris flows at the flanks of a tectonic graben system and are not at all related to any tsunami.

In this study, we discuss the origin of a chaotic, clastic deposit several meters thick that is preserved within the shallow marine sediments of the Pliocene La Portada Formation at Hornitos, northern Chile. Hartley et al. (2001) interpreted this coarse clastic bed as a deposit formed during backwash of a tsunami. Later on, the deposit was assigned to the Eltanin impact tsunami (Felton and Crook, 2003; Goff et al., 2012) that was triggered by a bolide impact in the southeast Pacific (Gersonde et al., 1997). We re-evaluate the involved depositional processes in the light of both tsunami and mass wasting events.

2. Background

2.1. Geological setting

The Coastal Cordillera of northern Chile in the region of Antofagasta (23°–24°S) forms a coast-parallel mountain range representing the westernmost continental regions of the central Andean fore-arc. It is positioned above the oceanic Nazca plate, which is being subducted eastward at an angle of c. 20° (Pardo-Casas and Molnar, 1987; Suárez and Comte, 1993). East of a 1–4 km wide coastal plain, the Coastal Cordillera rises steeply to altitudes of up to 2 km along the Great Coastal Escarpment (Paskoff, 1989; Ortlieb et al., 1996). In this region, the Coastal Cordillera mainly consists of Jurassic intrusives and volcanics that are covered by Cenozoic sediments (Ferraris and Di Biase, 1978; Pichowiak et al., 1990; Kramer et al., 2005). According to Hartley and Jolley (1995), a shallow-marine basin developed just west of the Great Escarpment during mid-Miocene to Pliocene times. At the basin margins alluvial, eolian and beach sediments developed. The clastic material that fed of the alluvial fans derived from the coastal escarpment that represented a paleo-cliff during the uplift of the Coastal Cordillera (Hartley and Jolley, 1995; Mather et al., 2014). These fan deposits are intercalated with shallow marine near-shore deposits of Pliocene to Pleistocene age (Ortlieb et al., 1996; Marquardt et al., 2004). Since then, the position of the alluvial fans and the shoreline did not change (Hartley and Jolley, 1995).

An exceptional morphological and structural feature along the coast of northern Chile is the Mejillones Peninsula just north of Antofagasta (Fig. 1). The peninsula protrudes from the main coastline by about 25 km. It is 55 km long and reaches altitudes of about 1000 m in

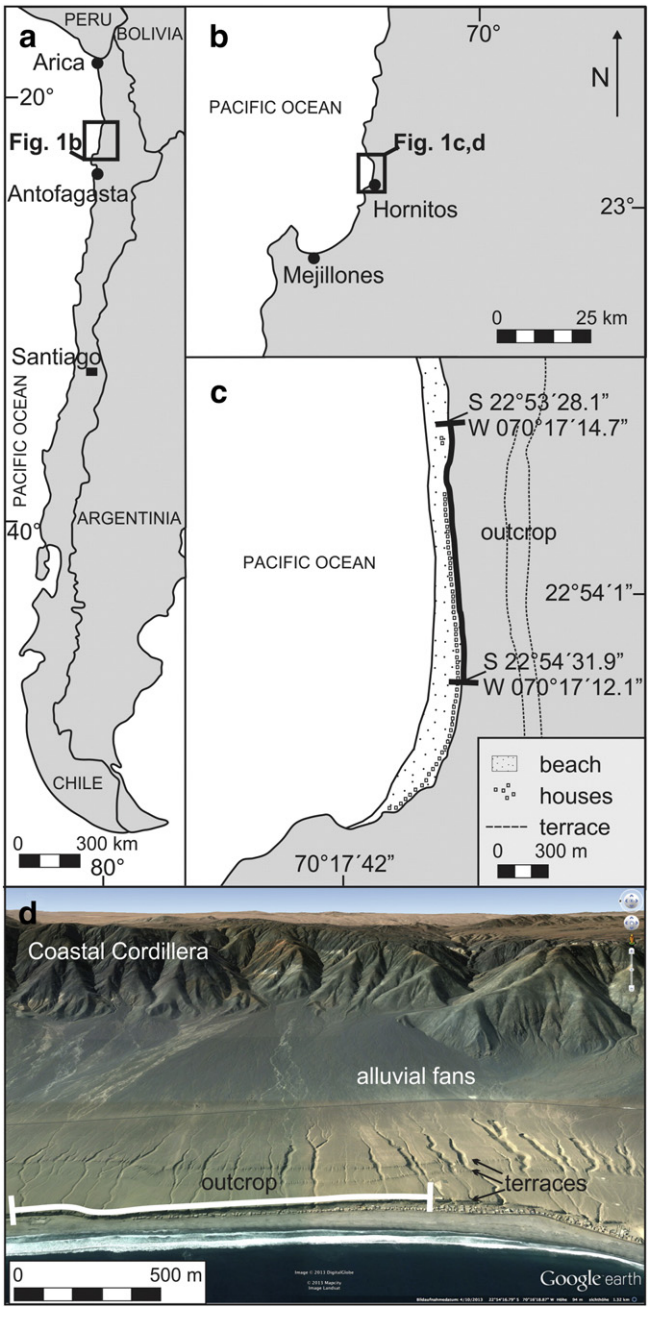

Fig. 1. Map of Chile a) depicting the location of the Mejillones Peninsula, and b) the location of Hornitos. c) Detailed overview of Caleta Hornitos and the coastal scarp where the assumed Pliocene tsunami backwash deposits (Hartley et al., 2001) crop out. d) Oblique aerial view (Google Earth, 2010) of the study site displaying the nearby Coastal Cordillera as source area for the magmatic rock slabs, the alluvial fans that transport coarse clastic material toward the sea, and the Pleistocene coastal terraces.

its southern part and about 300 m in the north. The main uplift of the Mejillones Peninsula started after 3.4 Ma and was on average between 0.4 and 0.5 mm y^{-1} since before 0.4 Ma, i.e. approximately double the average regional rate (Ortlieb et al., 1996; Victor et al., 2011). Uplift of both the Coastal Cordillera and the Mejillones Peninsula may already have started in the Miocene (Niemeyer et al., 1996).

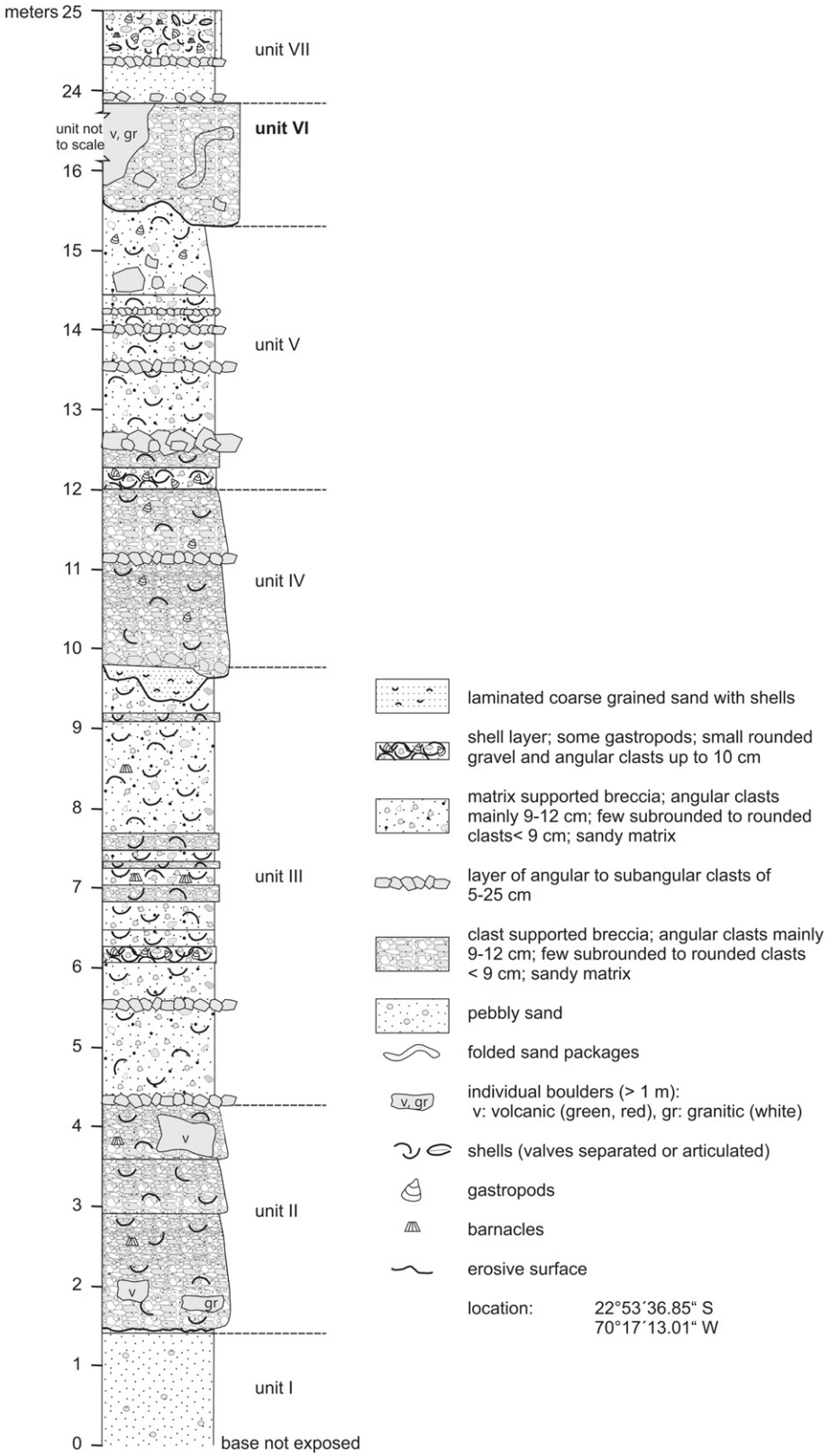

Fig. 2. Vertical profile of the outcrop at Caleta Hornitos. Note that Unit VI is not to scale.

Uplift of the forearc region north of Antofagasta resulted in the formation of a series of inboard stepping terraces. The oldest one is the 'Antofagasta Terrace' of Pliocene age which is in contact to the Great Coastal Escarpment at an altitude of + 100 m above present sea level (Martinez and Niemeyer, 1982). In the study area at Caleta Hornitos (Fig. 1), the youngest of three terraces is of Pleistocene age and rests atop a ~12 km long cliff with heights varying between 18 and 25 m above present sea-level (Ortlieb et al., 1996). The cliff, in turn, exposes shallow marine deposits of Pliocene age belonging to the La Portada Formation (Herm, 1969; Ferraris and Di Biase, 1978). The formation rests unconformably on andesites of the Early Jurassic La Negra Formation (Ferraris and Di Biase, 1978). It is an approximately 30–40 m thick succession of fine-grained shallow marine sandstones which contains a 7–10 m thick disorganized coarse-clastic layer (Fig. 2; Unit VI). Deposition of the La Portada Formation broadly coincided with the onset of increased uplift of both the Coastal Cordillera and the Mejillones Peninsula during the Pliocene which is supposed to be related to the subduction of an aseismic ridge (Hartley and Jolley, 1995; González et al., 2003; Victor et al., 2011).

Caleta Hornitos is located in Mejillones Bay, north of the Mejillones Peninsula (Fig. 1b), which acts as a barrier that restrains the influence of the dominant S-SW wind and associated fetch or storm swell. While the continental margin of northern Chile is generally characterized by a steep slope, Mejillones Bay resembles a gently sloping continental platform (Vargas et al., 2005). The bay is about 15 km wide and has a maximum water depth of around 125 m (Fig. 3b). The depth abruptly increases about 10–15 km off the coast.

2.2. Previous interpretation of the La Portada Formation at Caleta Hornitos

Hartley et al. (2001) were the first to interpret the sedimentary succession exposed along the coastal scarp at Hornitos as a result of a tsunami (Fig. 2). These authors attributed the succession to a shallow marine environment and correlated the sedimentary sequence with the Pliocene La Portada Formation (Ferraris and Di Biase, 1978). The alleged tsunamigenic deposit is a conspicuous coarse clastic bed (Unit VI) found within a sandstone sequence. The 7–10 m thick bed has an erosional basal contact and a local relief of 5–21 m along the basal unconformity surface (Hartley et al., 2001). Hartley et al. (2001) report local disruption of the lower contact by post-depositional soft-sediment deformation and that the largest angular to very angular andesitic basement clasts of the La Negra Formation incorporated in this unit are 5 m in diameter. The bed also contains very well-rounded granodiorite pebbles and cobbles, and shallow marine sandstone intraclasts of up to 10 m in diameter that originated from the underlying strata. These intraclasts occur both parallel to the bedding plane and as folded clumps. The sandstone intraclasts may be embedded in large-scale soft-sediment deformation features. The outsized boulders and intraclasts of several meters in diameter are found in a matrix of very poorly sorted fine to coarse grained sand that in parts shows poorly defined (sub)horizontal stratification. The matrix does not exhibit any sorting, grading or imbrication, but contains numerous shell fragments and some rounded granodiorite and andesite pebbles. At the top, Pleistocene marine terrace deposits truncate the Pliocene succession with an erosional unconformity (Ferraris and Di Biase, 1978).

Hartley et al. (2001) interpret the coarse clastic bed as a shallow marine tsunami backwash deposit. They base their interpretation on the presence of an erosional basal contact, outsized clasts, the exceptional thickness of the bed, and the fact that materials from different environments (shoreface and foreshore) are incorporated. The authors argue that the angular clasts reflect short transport distances of freshly quarried material from alluvial fans that was incorporated into the tsunami backwash together with rounded pebbles and cobbles that derived from nearby beaches. Finally, the sandstone intraclasts are interpreted as material being ripped off the underlying strata by the tsunami backflow. Hartley et al. (2001) note that the coarse clastic bed at Hornitos has an exceptional thickness, much thicker than any other submarine tsunami deposits documented in the literature (e.g., Shiki and Yamazaki, 1996; Massari and D'Alessandro, 2000). This is taken to imply that the sediments at Hornitos must have been created by an extraordinary tsunami event of great magnitude that happened during the Pliocene. Hartley et al. (2001) also state that a debris flow origin of the coarse clastic bed is unlikely. Their main arguments for this are i) the assumption that a debris flow would not result in the erosion and scouring of material from different depositional environments, such as the shoreface and foreshore, ii) a shallow marine debris flow would be reworked or eroded by subsequent storm and fair-weather processes, and iii) the respective deposits represent a depositional environment located about 3–5 km from the Pliocene coastal scarp, thus being several kilometers away from any drainage system that provides material for further seaward transport.

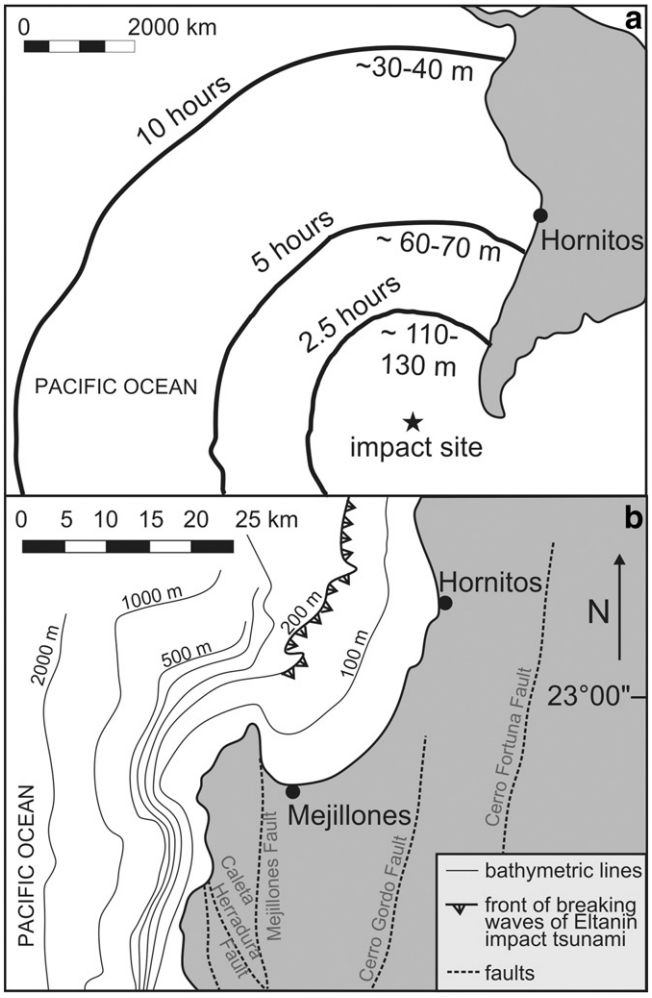

Fig. 3. The Eltanin impact. a) Location of the impact site and tsunami propagation including estimated wave heights in the Pacific Ocean (after: Ward and Asphaug, 2002). b) Bathymetry and distance of the breaking wave front of the impact-induced tsunami under consideration of the Van Dorn effect at Caleta Hornitos (after Korycansky and Lynett, 2005). Note that after the breaking of the tsunami offshore the onshore wave height would be reduced to 10–15 m (Korycansky and Lynett, 2005) in contrast to the previously assumed 50–60 m of Ward and Asphaug (2002).

2.3. The Eltanin impact and its tsunami

The Eltanin impact structure is located in the southern Pacific Ocean (Bellingshausen Sea; Gersonde et al., 1997) about 1500 km SSW of southern Chile (Fig. 3a). Kyte et al. (1981) discovered this impact structure by geochemical signatures in deep marine sediment cores.

Gersonde et al. (1997) estimated the impact age to 2.15 Ma; Frederichs et al. (2002) corrected the age to 2.511 ± 0.07 Ma. First estimates of the diameter of the asteroid between 0.1 and 4 km (Kyte and Brownlee, 1985; Gersonde et al., 1997) were refined by Shuvalov and Trubetskaya (2007) to a range between 0.5 and 2 km. The Eltanin event is the only asteroid impact known to have hit a deep ocean basin of 4–5 km water depth (e.g., Kyte et al., 1981; Gersonde et al., 1997).

Gersonde et al. (1997) proposed that the impact-related tsunami for a 1 km impactor would have wave heights of 20–40 m in the open ocean and run-up heights on the continental margins of South America and Antarctica 10–25 times higher than offshore (Fig. 3a). In the following years, the Eltanin impact tsunami was simulated for several impactor diameters (Table 1), such as 0.8 km (Weiss et al., 2006), 1 km (Ward and Asphaug, 2002; Shuvalov and Trubetskaya, 2007) and for a worst-case scenario of 4 km (Mader, 1998; Ward and Asphaug, 2002). In all computed scenarios a Pacific-wide tsunami was caused, though with different wave heights according to the size of the impactor (Table 1).

Mader (1998) was the first to model the tsunami as having been caused by a 4 km impactor. Modeled tsunami wave heights are about 80 m offshore southern Chile with onshore wave heights being 2–3 times higher (i.e., 160–240 m; Table 1). Ward and Asphaug (2002) calculated the worst-case scenario with an initial wave height of hundreds of meters close to the impact site. The tsunami would then reach the coasts of southern Chile and Antarctica with heights of up to 200–300 m and 50–100 m in central and northern Chile (Ward and Asphaug, 2002). Ward and Asphaug (2002) also show that a 1 km impactor would entail waves that are about five times smaller compared to the worst-case scenario, i.e. 40–60 m in southern Chile and 10–20 m in central and northern Chile (Table 1). In contrast, the model of Shuvalov and Trubetskaya (2007) using a 1 km impactor, documents that the highest tsunami wave hitting the closest shores of southern Chile would be less than 20 m. Finally, the study of Weiss et al. (2006), applying a 0.8 km impactor, presents the only model that considers a shoaling effect of the tsunami in shallow water depths. Including this effect, tsunami wave heights at the shore are reduced to about 2 m in a distance of 3000 km from the impact site.

For Hornitos, the worst-case scenario calculation by Ward and Asphaug (2002) suggests that the Eltanin impact tsunami hit the coastline at Hornitos about 6–6.5 h after the impact with a wave height of about 50–60 m (Fig. 3a). For a 1 km impactor, tsunami waves at Hornitos would be five times smaller, i.e. reduced to 10–12 m. In contrast, the study of Weiss et al. (2006) modeled wave heights of about 2 m for coasts in a distance of 3000 km from the impact site. Since Hornitos is located about 4300 km from the impact site, the onshore waves would consequently be <2 m.

Taking the higher end of the possible wave-height interval in the area of the Mejillones Peninsula, Felton and Crook (2003), as well as recent compilations by Goff and Dominey-Howes (2010) and Goff et al. (2012), speculate that the conspicuous coarse layer at Hornitos represents high-energy backwash currents of a Pacific-wide tsunami that was caused by the Eltanin impact (Fig. 3a). Recently, deposits at several other locations (Table 1) surrounding the Pacific Ocean were interpreted as evidence of the inundation by the Eltanin impact-tsunami (for a detailed list see Goff et al., 2012).

In Chile, a large number of sites that show unusual 'chaotic sediments' of Pliocene–Pleistocene age containing outsized boulders and large-scale fluid escape structures were also related to the Eltanin impact-tsunami (e.g., Goff et al., 2012). Most of the deposits are supposed to be coeval and hence were related to the same trigger (e.g., Le Roux and Vargas, 2005; Encinas et al., 2006; Walsh and Martill, 2006; Finger et al., 2007; Le Roux et al., 2008). Strikingly, not all of the original papers relate these deposits to a tsunamigenic origin. In particular the deposits described by Walsh and Martill (2006) and Finger et al. (2007) were linked to the Eltanin impact tsunami by third parties (e.g., Goff et al., 2012).

3. Methods

A complete vertical section of the exposed terrace front (ca. 25 m high; 2 km long) was studied at Caleta Hornitos (Figs. 1c, d, 2). Thickness, grain size, and grading trends of the sediment layers were measured and described in the field. The lithology of the incorporated clasts, their roundness or angularity and the composition of the matrix were documented. Additionally, the abundance of marine organisms (e.g., shells, barnacles, gastropods, bones) including their state of preservation (articulated, broken or fragmented) were recorded. Samples for microscopic analysis were taken at different levels within the vertical profile. These samples were examined with a reflected-light microscope. As for the macroscopic particles, the preservation condition and abundance of the microorganisms (e.g., foraminifera, ostracods) were described. Thin sections of hand specimen taken from boulders incorporated in the deposits were prepared for petrographic analysis under the polarized light microscope (Leica DMRX).

Table 1
Overview of modeled off- and onshore tsunami wave heights for different diameters of the Eltanin impactor. The site of Hornitos is located about 4300 km from the impact site. Hornitos would be reached by the tsunami ca. 6–6.5 h after the impact according to the simulations of Ward and Asphaug (2002). It needs to be noted that only Weiss et al. (2006) include a shoaling effect of the tsunami in shallow water.

Reference	Diameter of impactor	Offshore tsunami wave height	Onshore tsunami wave height
Gersonde et al. (1997)	1 km	Southern Pacific 20–40 m Northern Pacific 5–10 m	10–25 times higher than offshore
Mader (1998)	4 km	Chile 80 m Drake Passage 65 m New Zealand 40 m Alaska 30 m Hawaii 28 m California 20 m Japan 8 m	2–3 times higher than offshore
Ward and Asphaug (2002)	1 km		Southern Chile[a], Antarctica 40–60 m Chile[b] 10–20 m Hornitos ca. 10–12 m
	4 km	Some 100s of meters	Southern Chile[a], Antarctica 200–300 m Chile[b] 50–100 m Hornitos ca. 50–60 m Central America 35–40 m New Zealand 60 m
Weiss et al. (2006)	0.8 km	200 m at impact site	<2 m 3000 km from impact site
Shuvalov and Trubetskaya (2007)	1 km	Some 100s of meters	Southern Chile[a] ca. 20 m

[a] Southern Chile: from the southernmost tip of Chile (Tierra del Fuego) to Chiloé.
[b] Chile: central to northern Chile; from Chiloé to Arica.

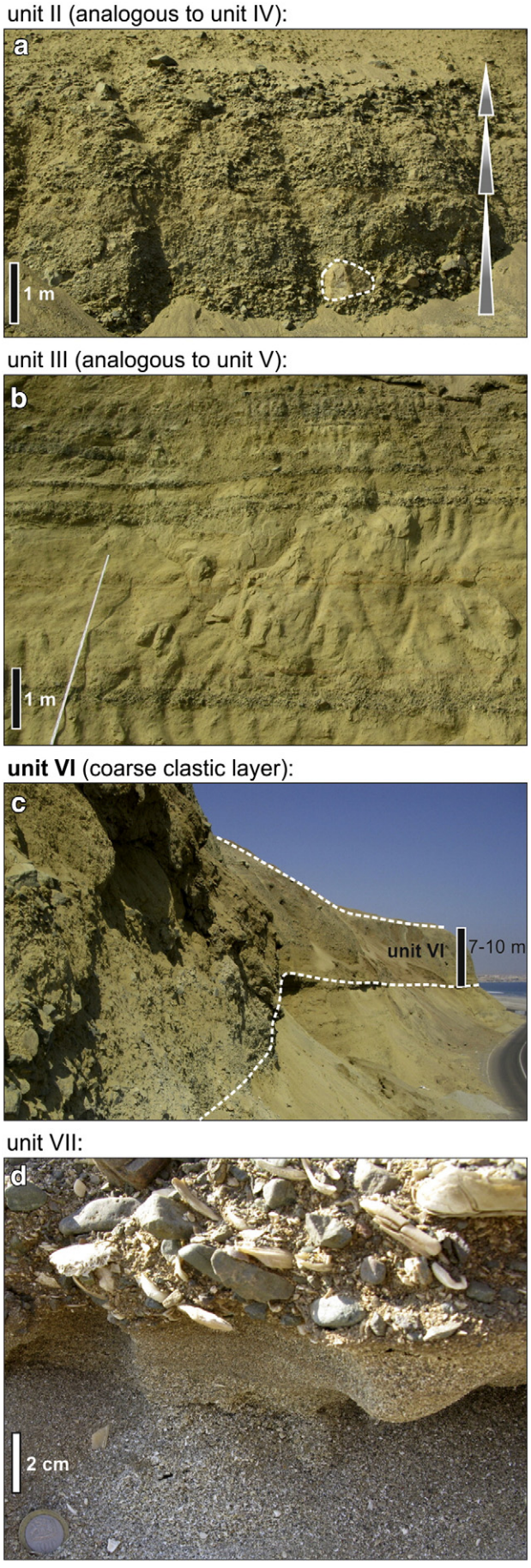

4. Results

4.1. Description of the sedimentary succession at Caleta Hornitos

The vertical profile exhibits 36 macroscopically recognizable sediment beds that can be subdivided into seven depositional units (Figs. 2, 4). The lowermost Unit I has a thickness of at least 1.4 m and is made of a pebbly sandstone. Its base is not exposed. The very well rounded pebbles are max. of 4 cm in diameter and occur in a semi-lithified matrix composed of silt and fine sand.

Above this pebbly sandstone, Unit II consists of three normally graded beds (1.5 m, 1.0 m, 0.7 m; Figs. 2, 4a). These beds have erosive bases and are clast-supported breccias composed of angular (rarely slightly rounded) clasts of 0.5–9 cm within a sandy matrix. The sediments contain abundant shell fragments (mainly pecten), some barnacles and a few small bone fragments (Fig. 5a, b). Distinct large angular boulders of granitic and volcanic lithology measuring 40 × 25 cm, 50 × 20 cm and 75 × 50 cm are present (Fig. 4a). Unit II is much stronger lithified than the pebbly sandstone of Unit I.

Unit III is about 5.5 m thick and composed of several beds of a matrix-supported breccia with some intercalated clast-supported breccia layers (Figs. 2, 4b). The matrix-supported breccia has a silty to sandy matrix that contains clasts of up to 10 cm. The bigger clasts are mainly angular, whereas some of the smaller ones are subrounded. The amount of incorporated shell fragments and remains of barnacles varies among layers. The clast-supported breccia layers, in turn, are 10–20 cm thick, contain shell fragments, angular clasts (<10 cm) and smaller subrounded clasts. At the base of Unit III and at 1.1 m there occurs two conspicuous layers of up to 15–20 m thickness consisting of very angular clasts. The bed thicknesses are nearly equal to one clast diameter and there is hardly any sandy interstitial material. About 6 m from the base of the outcrop and within Unit III, a 20 cm thick shill layer is present. It contains numerous shell fragments and gastropods, as well as angular basement clasts of up to 10 cm in diameter and some smaller rounded pebbles.

The following Unit IV is about 2.2 m thick and similar to Unit II. It is composed of two graded layers (1.3 and 0.8 m thick) that are separated by a clast-supported breccia with a thickness that is equal to a clast diameter of about 12 cm (Figs. 2, 4a). The breccia is almost free of matrix between the clasts. The two graded layers are clast-supported and have clasts of about 12 cm at the base and 3 cm at the top. The layers contain few shell fragments and gastropods. The base of the lowermost breccia is erosive and undulating. The erosional scours are filled with laminated sand that is at the top enriched in small (<1 cm) shell fragments.

Unit V consists of matrix-supported breccias similar to Unit III. It begins with a 25 cm thick layer of angular clasts which also is rich in shell fragments (Figs. 2, 4b). The overlying breccia layer with shell fragments is intercalated by four coarse layers with hardly any interstitial sand, and thicknesses are equal to one clast diameter (25 cm, 15 cm, 12 cm, and 5 cm, respectively from bottom to top). The uppermost 1.2 m of this unit exhibits weak normal grading trend. This part contains slightly more shell fragments and gastropods than the lower underlying. The biggest angular clasts at the base of the graded unit are 40 × 30 cm.

Unit VI is the principal target unit of this study (Figs. 2, 4c). The unit is a clast-supported breccia (average clast size 5–15 cm) with a silty to sandy matrix and few incorporated biota remains. It has an undulating base and exhibits scouring of up to 3–6 m in relief. Its thickness is 7–10 m, as it varies along the cliff front due to the erosive nature of its base. The majority of clasts are angular grayish-green volcanics, and only a minor clast fraction is made up of subrounded to rounded

Fig. 4. Overview of the different units. a) Unit II consisting of several graded clast-supported breccia layers and some bigger boulders at the base, b) Unit III (analogous to Unit V) depicting sand layers with some intercalating breccia layers, c) Unit VI which Hartley et al. (2001) assigned to a tsunamigenic origin, and d) rounded clasts and organism remains within the sandy matrix of Unit VII.

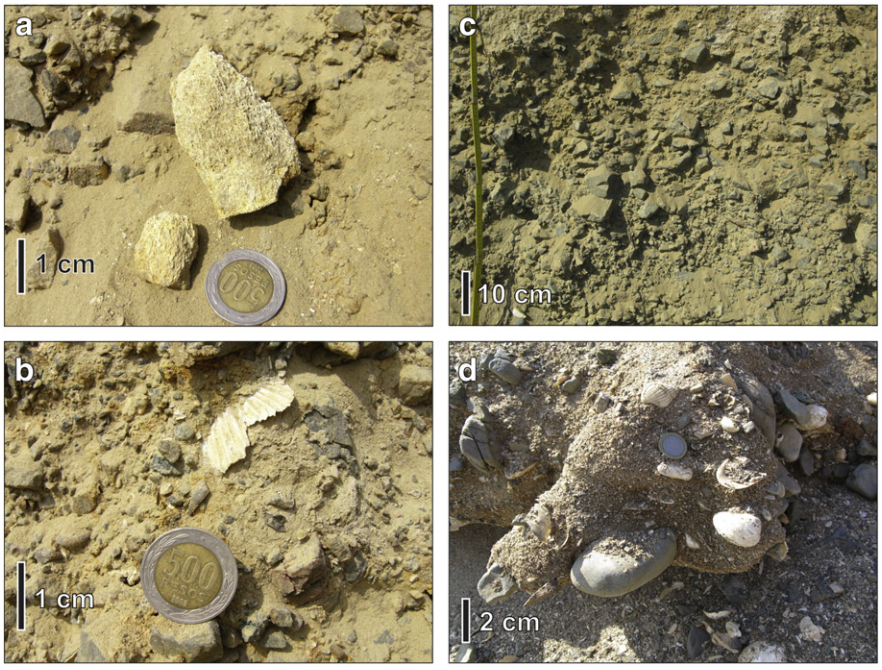

Fig. 5. Detailed view of components and sedimentary features found within the different units. a) Bone and b) shell fragments of Unit II. c) Typical clast-supported breccia. d) Mixture of rounded pebbles, unfragmented gastropods and broken shells of Unit VII.

brownish-red basaltic rocks. Within the vertical succession of Unit VI no grading is present. Outsized clasts and large-scale sedimentary structures occur along the cliff section at Caleta Hornitos.

The uppermost Unit VII is separated from Unit VI by a sharp disconformity (Figs. 2, 4d, 5d). The erosional surface is planar and can be traced as a distinctive horizontal line along the entire cliff front, e.g. cutting the top of outsized boulders. Unit VII has some angular clasts (up to 15–20 cm diameter) at its base and is overlain by a several decimeters thick package of laminated sand, rich in small shell fragments (<0.5 cm). Another single clast layer of about 15 cm thickness separates the laminated sand from an overlying sand layer that consists of a chaotic mix of fossils and clasts. The clasts are mainly subrounded to rounded. Some of them have barnacles attached to the surface. The layer is full of gastropods, barnacles, shell fragments, single shell valves (up to 10 cm), as well as articulated shells. This unit represents the surface of the most seaward coastal terrace.

4.2. Large-scale features of the coarse clastic layer (Unit VI)

The average thickness of the clast-supported breccia of Unit VI is 7–10 m. The unit can be traced for nearly 2 km along the coastal scarp at Hornitos before it pinches out at the northern and southern ends of the outcrop (Fig. 6a). Unit VI exhibits a variety of large-scale erosional and depositional features (Figs. 6, 7). However, horizontal or vertical sorting trends are not present. Locally, the contact to the underlying Unit V is erosional with scour depths of up to 3–6 m (Figs. 6b–d, 7a). In some cases the scours cut into horizontally laminated layers of the underlying units.

Boulders and large elongated, oblate rock slabs can reach up to several tens of meters in length and about 10 m thickness (Fig. 7). Some slabs are broken, with the isolated pieces being displaced relative to each other (Fig. 6b) or separated by sand intrusions (Fig. 7b). Boulders and rock slabs do not cut or impact into the underlying Unit V, but are rather floating within the matrix of the breccia layer.

Soft-sediment deformations and sand injections are visible at several locations along the outcrop (Fig. 6c–f). Sandstone clasts and lumps are in some places deformed and folded (Figs. 6d–f, 7c). Locally, deformed sand is interfingering with the breccia (Fig. 6c).

The top of Unit VI displays a sharp erosional contact to Unit VII. This unconformity is best developed where the surfaces of large boulders and rock slab are horizontally truncated by the overlying Pleistocene marine terrace deposits (Figs. 6e, 7a, c).

5. Discussion

The coarse clastic bed of Unit VI was first interpreted as the backwash deposit of a large Pliocene tsunami (Hartley et al., 2001). Later, the conspicuous layer was attributed to the Eltanin impact (Felton and Crook, 2003; Goff and Dominey-Howes, 2010; Goff et al., 2012) which caused a Pacific-wide tsunami that is supposed to have severely affected the coasts of southern America (Ward and Asphaug, 2002). Contrastingly, we suppose that both the general interpretation of the unit as a tsunami backwash deposit and the linkage to the Eltanin impact are highly speculative and lack convincing evidence and data.

We argue that Unit VI needs to be reinterpreted first of all because of the differences to the original description by Hartley et al. (2001) that does not include large-scale depositional features. Secondly, several sedimentary features and the overall tectonic background and depositional setting are neither supporting a tsunami origin of the unit, nor any relation to the Eltanin impact event. These arguments are (1) the biostratigraphic age of Unit VI in relation to the Eltanin impact (Powell et al., 2005a,b), (2) the lack of impact-related constituents in comparison to other Chilean sites that are also supposed to be related to the Eltanin impact (Le Roux et al., 2008), (3) the oversimplification of previous modeling attempts of the Eltanin impact tsunami (Ward and Asphaug, 2002), and (4) the lack of analogous submarine tsunami features caused by recent tsunami (e.g., Noda et al., 2007; Di Geronimo et al., 2009; Feldens et al., 2009; Paris et al., 2010; Feldens et al., 2012; Kawagucci et al., 2012; Arai et al., 2013).

5.1. Differences to the original description by Hartley et al. (2001)

We agree with Hartley et al. (2001) that no obvious trend of grading or sorting can be observed in Unit VI. However, our description of the sedimentary succession exposed at Hornitos differs significantly from

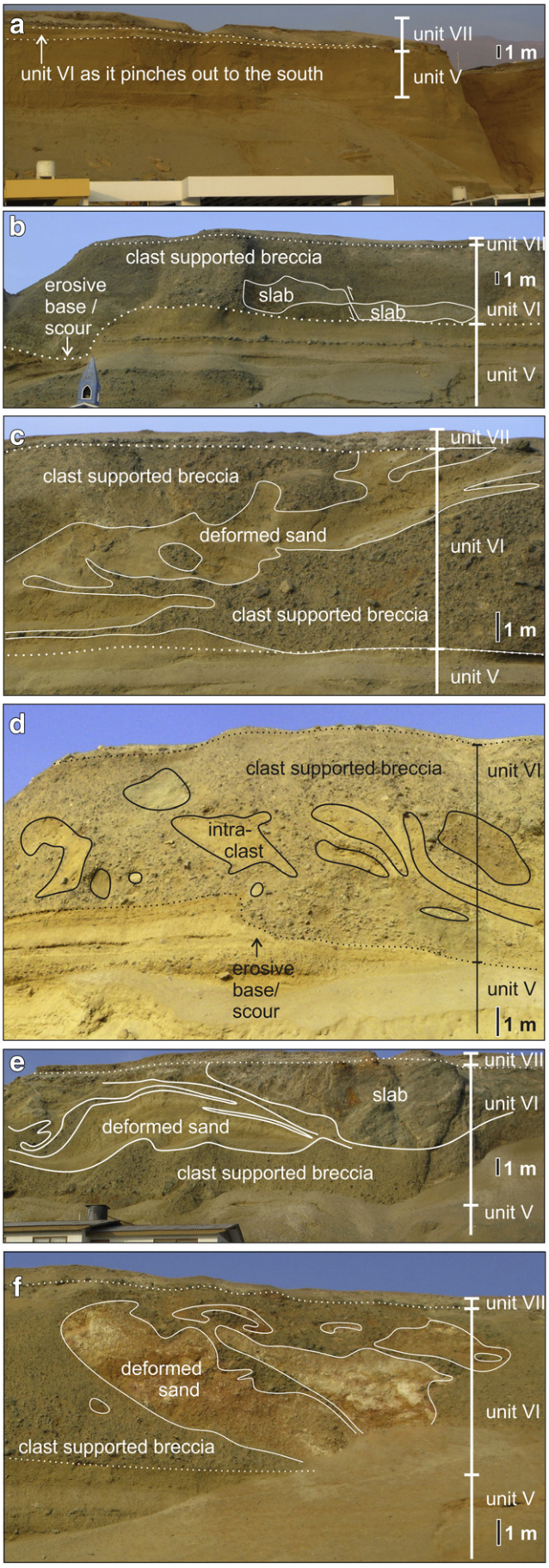

the documentation given by Hartley et al. (2001). The main differences are:

i) The ~25 m high vertical succession cannot be described as 'a succession of yellow sandstones that contain a shell-rich conglomerate bed'. Instead, the sequence can clearly be subdivided into seven units (Figs. 2, 4). Only the lowermost pebbly sandstone (Unit I) more or less matches the description by Hartley et al. (2001). Furthermore, the proposed event bed (Hartley et al., 2001) is not the only coarse clastic, shell-rich bed within the succession, but one of several beds. We agree with Hartley et al. (2001) that the bed has an exceptional thickness of 7–10 m compared to the other coarse clastic beds the thicknesses of which are not exceeding 1.5 m.

ii) Along the entire cliff front we were not able to find any erosional scours or relief of up to 21 m depth, as reported by Hartley et al. (2001). Instead, observed scour depths at the base of Unit VI do not exceed 3–6 m (Figs. 6b–d, 7a).

iii) Hartley et al. (2001) denote the event bed as a conglomerate. We propose that the term conglomerate does not properly describe the sedimentary inventory of the unit. Instead, subangular to angular clasts dominate. Therefore, classifying this bed as a clast-supported breccia with a silty to sandy matrix that contains a few organism remains in addition to some outsized rock slabs seems more appropriate.

iv) Hartley et al. (2001) document sandstone intraclasts (ca. 10 m diameter) that are partly folded and occasionally surrounded by large-scale soft-sediment deformation features (Figs. 6c–f, 7c). They attribute these features to sediment deformation of the underlying unit. We agree with this observation. However, the previous study does not mention the presence of large-scale sand dykes that cut through the rock slabs (Fig. 7b). These structures either indicate the intrusion of unconsolidated sand from the underlying unit into fractures of the rock slabs and finally breaking the slabs, or a catastrophic deposition of the rock slabs during which they broke and sand was then squeezed into the cracks.

v) The maximum clast size for basement boulders given by Hartley et al. (2001) is 5 m. Tracing the conspicuous bed along the cliff front shows that much bigger rock slabs of up to several tens of meters are commonly incorporated into the unit (Fig. 7). Furthermore, these boulders and slabs do not erode or impact into the underlying unit, but are rather floating within Unit VI.

vi) The description of Hartley et al. (2001) includes the observation that 'some reworking' of the upper part of the coarse clastic bed occurred because it is abruptly overlain by shoreface sandstones. Hartley et al. (2001) argue that this erosion entails the lack of a graded unit at the top of the tsunami succession, which would represent the deposition of fine sediment during the waning flow of the tsunami. We agree with this observation and interpretation. Nevertheless, we argue that the erosion, truncating the alleged event bed, seems to be of much greater extent than considered by Hartley et al. (2001). We attribute this intense erosion to the fact that huge basement slabs with irregular shape show a sharp, horizontal erosional surface (Fig. 7). The action that led to the erosion of the top of those basement boulders must be classified as strong, possibly long term processes instead of 'some reworking' as stated by Hartley et al. (2001).

Fig. 6. Large-scale sedimentary and erosional features within Unit VI. a) Pinching out of Unit VI at the southern side of the outcrop. b) Large broken and displaced rock slab. c) Clast-supported breccia interfingering with deformed sand. Note the erosive character of the upper contact. d) Partly folded sandstone clasts. e) Large rock slab and deformed sand within the clast-supported breccia. The top of the rock slab has a sharp, erosive surface. f) Partly folded sandstone clasts within the clast-supported breccia.

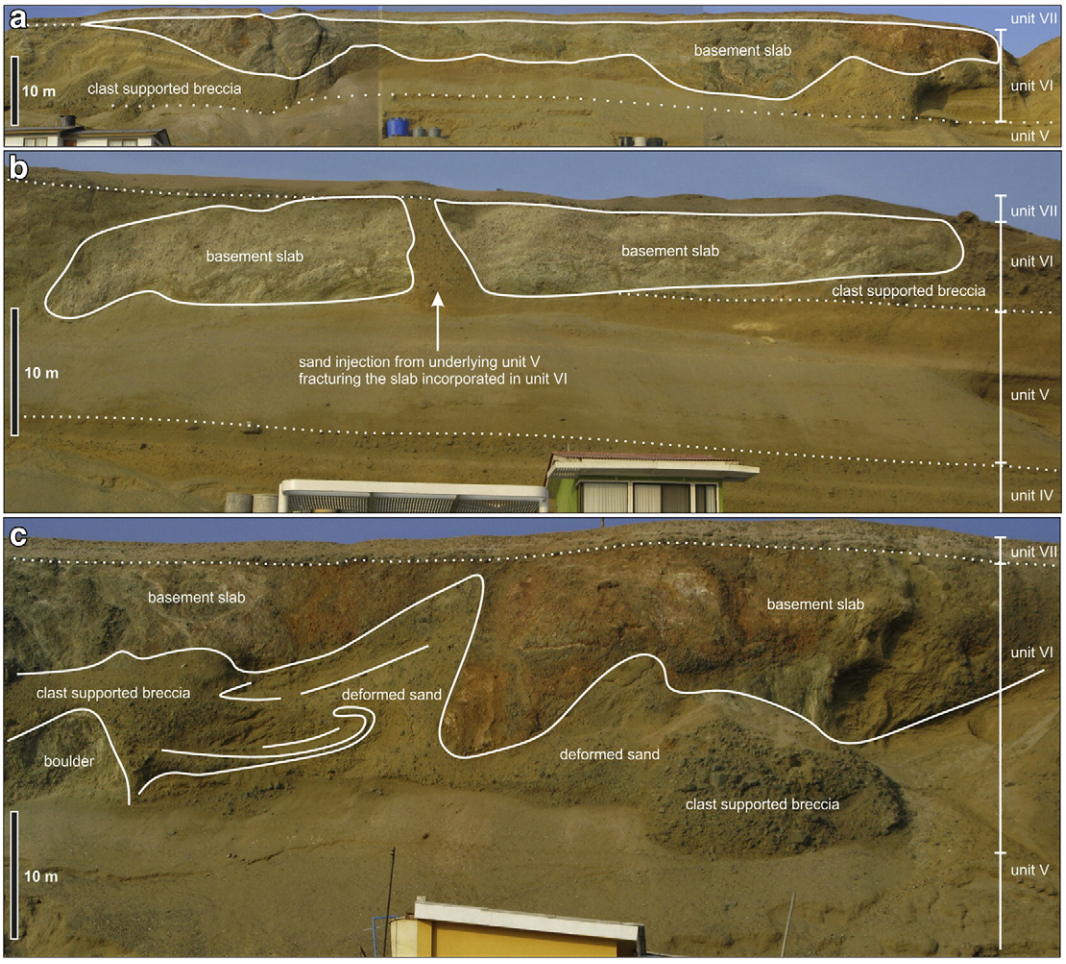

Fig. 7. Large rock slabs incorporated in Unit VI. a) Largest unbroken basement slab. Note the erosive contact to the overlying unit. b) Basement slab fractured by sand injections from the underlying Unit V. c) Basement slab with erosive top and deformed sand within the clast-supported breccia.

5.2. Arguments against a (Eltanin impact) tsunami origin

(1) The age of the La Portada Formation relies on planktonic foraminifera such as *Globigerinoides conglobatus* and *Neogloboquadrina acostaensis* that point to an early to middle Pliocene age (5.1–2.8 Ma; Powell et al., 2005a,b). Deposition of the La Portada Formation including the coarse event bed thus slightly predates the Eltanin impact (2.511 ± 0.07 Ma; Frederichs et al., 2002). At Hornitos, any potential Eltanin impact deposits might have occurred in the sedimentary gap and stratigraphic hiatus between Unit VI and the Pleistocene terrace deposit (Unit VII) that is represented by a significant disconformity (Figs. 6, 7). However, both the Eltanin event (Frederichs et al., 2002) and the La Portada Formation (Powell et al., 2005a,b) lack absolute age data and instead rely on less precise biostratigraphic data (Le Roux et al., 2008). Additionally, not only Unit VI, but the entire succession at Hornitos resembles sediment beds of reworked and mixed material from sources of various environments and ages that makes complicates the establishment of a detailed biostratigraphy. Hence, the precision of the available impact and deposit ages is questionable.

(2) Goff et al. (2012) point out that an outcrop of the Pliocene Ranquil Formation, about 1600 km south of Hornitos (Le Roux et al., 2008), is the closest occurrence of another possibly Eltanin impact connected tsunami sediment. Other than Hornitos, the Ranquil Formation has a poorly defined biostratigraphic age of 5.3–1.8 Ma (Le Roux et al., 2008) and thus may in fact cover the time interval of the Eltanin impact (Frederichs et al., 2002). The greatest difference to the coarse bed in the La Portada Formation is the presence of partially molten quartz and glass particles in the sediments of the Ranquil Formation that may indeed be related to an impact (Le Roux et al., 2008).

(3) Regardless of the still poorly constrained size of the impactor, it is widely accepted that the Eltanin impact was able to cause a Pacific-wide tsunami (Table 1; Fig. 3a). Ward and Asphaug (2002) note that a more conservative size of 1 km entails tsunami wave heights in central Chile that are about five times smaller (10–20 m) compared to the worst-case scenario of a 4 km impactor (50–100 m). However, Korycansky and Lynett (2005) note that the linear shallow-water propagation model of Ward and Asphaug (2002) is not applicable for deep sea-impacts and does not include the Van Dorn effect. Compared to earthquake-induced tsunamis, an impact-generated tsunami has shorter wavelengths and higher amplitudes in the open ocean, but will decay much quicker as soon as it approaches shallow water (e.g., Melosh, 2003; Wünnemann et al., 2010, 2011). The Van Dorn effect takes this shoaling into account. Thus, the tsunami height will be significantly reduced and the tsunami will break several kilometers offshore in the outer shelf region. Onshore tsunami wave heights will be significantly smaller. Korycansky and Lynett (2005) argue that for steep continental margins with only narrow shelf areas, i.e. a typical Pacific active margin bathymetric profile such as in northern Chile, an impact-induced tsunami will break 3–17 km offshore. Thus, a deep-water wave of 10 m wave height will break 3–7 km offshore, a wave of 20 m 5–10 km offshore, of 50 m 10–14 km offshore and of 100 m 15–18 m offshore (Korycansky and Lynett, 2005). Applied to the Eltanin impact at Hornitos, this would imply that a worst-case scenario wave of 50–60 m will break about 10–14 km offshore and a more conservative

wave estimate of 10–12 m will entail breaking 3–7 km offshore. Assuming that the coastline did not significantly shift since Miocene, most probably Pliocene times (Hartley and Jolley, 1995), a distance of about 10 km offshore would roughly correspond to the current 200 m bathymetric line (Fig. 3b).

The breaking of the tsunami in outer shelf regions creates a wide zone of large-scale turbulences with strongly nonlinear wave behavior (Korycansky and Lynett, 2005). This energy will dissipate quickly during the passage of the wave over the shelf and reduce the onshore wave height to about 30% of the offshore wave height (Melosh, 2003; Korycansky and Lynett, 2005). For Hornitos, the onshore wave height would then be about 18 m for a 4 km impactor and 4 m for a 1 km impactor. Weiss et al. (2006), using a 0.8 km impactor, modeled wave heights of about 2 m for coasts in a distance of 3000 km from the impact site. Since Hornitos is located about 4300 km from the impact site, the onshore waves would consequently be <2 m. Additionally, the main uplift of the Mejillones Peninsula started at about 3.4 Ma (Ortlieb et al., 1996; Victor et al., 2011). Thus, at the time of the Eltanin impact (2.511 ± 0.07 Ma; Frederichs et al., 2002) the peninsula already existed and would likely have acted as a barrier that weakened the impact of waves approaching Mejillones Bay from the south to southwest (Figs. 1, 3b).

Despite the discussion on impactor size and both off- and onshore tsunami wave heights, there is also the need to consider that the Eltanin impact did not cause a far-field tsunami at all. Gisler et al. (2004, 2011) and Wünnemann et al. (2007, 2010) argue that during deep water impacts amplitudes of the nonlinear tsunami waves will attenuate inversely already at proximal distances (ca. 50–150 km) from the impact site. In contrast to shallow water impacts, the initial rim waves that are generated during bolide impact into the ocean, will decay almost immediately and can be neglected in the far field for deep water impacts (Wünnemann et al., 2010). The secondary collapse waves that are generated during the collapse of the central peak of water within the crater are highly nonlinear and will also dissipate quickly (Wünnemann et al., 2007, 2010).

An indirect consequence of large impacts is seismic shaking. In case of the Chicxulub impact (diameter of the impactor larger than water depth), the accompanied seismic shaking is assumed to equal the effects of a M_w 10–13 earthquake (Norris et al., 2000; Day and Maslin, 2005). Boslough et al. (1996) estimated that such an event caused ground motion in excess of 1 m within 7000 km from the impact site, triggering marine mass failures and platform or margin collapses (e.g., Bralower et al., 1998; Klaus et al., 2000; Norris et al., 2000; Kiyokawa et al., 2002; Goto et al., 2008). Such seismic effects did possibly not accompany the Eltanin impact because it was a deep-sea impact that is not proven to have created a sea floor crater. Thus, impact-related shaking is to be excluded as indirect trigger of Unit VI at Hornitos.

(4) Wünnemann et al. (2010, 2011) concluded that tsunamis caused by marine impacts will not reach a coastline thousands of kilometers away with immensely destructive power and that they will not cause far-field effects as severe as the 2004 Indian Ocean tsunami. Instead, compared to recent tsunami, an onshore tsunami wave height of about 18 m, as calculated for the worst-case scenario of the Eltanin impact tsunami, does not represent an extraordinary event; this applies even more for more conservative onshore wave heights of 4 m or less. For instance, both the 2004 Indian Ocean tsunami (e.g., Borrero, 2005; Lavigne et al., 2009), and the 2011 Tohoku tsunami (e.g., Hooper et al., 2013) had observed local onshore flow depths of 30–35 m. Reconnaissance surveys that were conducted after these two events indeed observed marine tsunami backwash deposits (e.g., Feldens et al., 2009; Paris et al., 2010; Feldens et al., 2012; Kawagucci et al., 2012; Haraguchi et al., 2013), but those are very dissimilar to the deposit at Hornitos which is much thicker and contains much larger clasts.

A study of Paris et al. (2010) after the 2004 Indian Ocean tsunami in Aceh documented an interference of both the tsunami run-up and backwash down to at least 25 m water depth. The backflow was able to transport boulders of about 15 m diameter to 1.95 km offshore and of 5.5 m to 2.4 km offshore; larger boulders and rock slabs, like the ones in Hornitos, were not moved. Backwash flow velocities necessary to move the largest boulders were 7 m/s in a distance of 3.2 km from the coast; highest flow velocities are proposed to have reached 8–21 m/s. While the backwash redeposited boulders and large anthropogenic debris not more than about 2–3 km offshore, the finer-grained sandy to muddy sediment bypassed the shallow marine environment and was deposited farther offshore. Such a transfer of the suspended sediment seems to be a typical process directly linked to tsunami backwash, and is in sharp contrast to a debris flow that will move material of different grain size en masse and deposit coarse clastic components within a finer-grained matrix, as present in Hornitos. If one wanted to maintain the interpretation of Unit VI at Hornitos as a tsunami deposit, one needs explain process-wise why it differs so significantly from recent examples.

There are several examples of ancient marine sedimentary units interpreted as the result of a tsunami (e.g., Le Roux and Vargas, 2005; Schnyder et al., 2005; Brookfield et al., 2006; Goto et al., 2008; Le Roux et al., 2008). Some of them are similar in thickness to Unit VI and similarly include huge boulders and rock slabs. The high-energy hydrodynamics required to form such marine chaotic block-in-matrix sediments could be taken to imply that tsunami were of greater magnitude in the past when compared to recent events. A comprehensive literature review of chaotic block-in-matrix sediments would also involve a re-evaluation of the origin of other such deposits including sedimentary mélanges or olistostromes (e.g., Abbate et al., 1970; Festa et al., 2010).

On a regional scale, several Mio- to Pliocene sedimentary successions exposed along the coast of Chile and being interpreted as marine tsunami deposits need to be reconsidered. The interpretation of proposed shallow marine tsunami deposits described by Cantalamessa and Di Celma (2005) has already been revised (Bahlburg et al., 2010). Our study at Hornitos seems to be the second case in which, considering sediment features and the depositional setting, a tsunamigenic origin can be excluded. Therefore, the depositional processes of other proposed tsunami deposits need likewise to be reconsidered, at least in coastal outcrops in Chile, but most possibly also worldwide.

5.3. Reinterpretation of the depositional environment at Hornitos

Taking the above listed arguments into account, we question the former interpretation as a shallow marine backwash tsunami deposit and argue for a marine debris flow origin of Unit VI. A distinction of such submarine mass wasting deposits in terms of their triggering mechanisms is challenging and current knowledge may not allow such discrimination in every case. This is because sediments rarely record the interrelation of earthquakes, slides and tsunami (Shiki, 1996; Shiki and Tachibana, 2008; Shanmugam, 2012). An earthquake can directly generate a tsunami or indirectly by triggering a submarine slide which then may trigger a slide-induced tsunami, such as reported from the Grand Banks event (Heezen and Ewing, 1952), the Papua New Guinea event (Tappin et al., 1999), and Lake Lucerne (Strasser et al., 2011). On the other hand, a submarine slide that can induce a tsunami may occur without a previous earthquake (e.g., Locat et al., 2004; Lo Iacono et al., 2012; Tappin, 2012). Offshore Chile submarine slides are common features along the Chilean continental margin. Large possibly tsunami triggering slides of Pleistocene to Holocene age were reported by Völker et al. (2009) and Geersen et al. (2011). Apart from earthquakes, such slides may be triggered by, among others, tectonic uplift, oversteepening of the slope, sea level rise, excess pore pressure, destabilization by dissolving gas hydrates, and the presence of weak layers (Masson et al., 2006). In all cases proximal and distal mass wasting units will be deposited that may look similar to deposits that are related to earthquakes or tsunami. Additionally, in shallow marine environments reworking of all those types of sediments by fair-weather and storm waves should be expected (Weiss and Bahlburg, 2006). For

a comprehensive discussion on the mechanics and hydrodynamic processes of debris flows, and types of mass wasting deposits and their sedimentary characteristics we refer to Mulder and Cochonat (1996), Mulder and Alexander (2001), Masson et al. (2006), Parsons et al. (2007) and Talling et al. (2012).

The sedimentary features documented in Unit VI at Hornitos are consistent with typical large-scaled marine debris flow deposits that are interbedded in frequent, but less energetic shallow marine mass-wasting deposits of much smaller scale. Flores (1956) notes that such chaotic block-in-matrix sediments contain intra- and extraclasts of different ages. At Hornitos, large rock slabs from the basement, sandstone clasts from the underlying strata, angular clasts from alluvial fans, as well as shell material from the nearshore zone and beach were incorporated into the deposit. The large basement rock slabs floating in the matrix and the fact that only minor erosion is visible at the base of the coarse-clastic bed may suggest that hydroplaning played a significant role during the transport (Abbate et al., 1970; Mohrig et al., 1998). A basal layer consisting of an overpressured mixture of loose sediment and water may also explain the presence of sand injections (Fig. 7b; Mohrig et al., 1998). Flow internal shear is represented by plastic soft-sediment deformation (Festa et al., 2010; Pini et al., 2012) both of sandstone clasts that were not or only poorly consolidated prior to the transport (Fig. 6d), and by the interfingering of deformed sand and the clast-supported matrix (e.g., Fig. 6c). Unit VI itself does not depict any bedding or trends (i.e., grading, sorting) which is also typical for debris flow deposits (Flores, 1956; Abbate et al., 1970).

Considering the tectonic background of the north Chilean active margin including the rapidly uplifting Mejillones Peninsula, the most conclusive interpretation of Unit VI is a debris flow deposit that was triggered by a local earthquake. A major phase of tectonic uplift that affected both the Coastal Cordillera and the Mejillones Peninsula started during the Pliocene (Hartley and Jolley, 1995; Niemeyer et al., 1996; González et al., 2003; Victor et al., 2011). The fast emergence of the Coastal Cordillera entailed an increase in slope angle, destabilizing coastal cliffs and continental slopes (González et al., 2003). Mather et al. (2014) report on a number of subaerial landslides and rock avalanches of Plio-/Pleistocene age that terminated into the Pacific; the closest site being just 10 km north of Caleta Hornitos. They also note that such large-scale landsliding is capable of transferring sediment on regional scale into offshore environments. One example is the El Magnifico landslide that generated a ca. 8 m thick debris fan consisting of breccias and blocks deriving from local bedrock, and reaching some 5 km offshore (Mather et al., 2014). Another slide deposit exposed along the coastal cliff of Caleta Verde (ca. 270 km north of Hornitos; Mather et al., 2014) has a strikingly similar appearance to Unit VI at Hornitos, being 6.5 m thick, preserved within shallow marine sediments, consisting of breccias and blocks, and being truncated by the lower marine terrace. Hence, a reinterpretation of Unit VI as a mass wasting deposit would be supported by several similar features in the region that were deposited in the same ways.

Repeated slope failures were most probably triggered by local earthquakes, which are supposed to be the most efficient triggers (Maltman, 1994; Camerlenghi and Pini, 2009; Festa et al., 2010). At Hornitos, smaller scale mass wasting deposits (Units II, III, IV, V) are probably the result of minor failures that are typical for emerging coastlines like northern Chile (Geersen et al., 2011), whereas the shallow marine coarse-clastic Unit VI is the result of a large-scale cliff collapse or retrogressive slide. The fact that the Unit VI contains components from onshore and nearshore environments, implies that the failure comprised both the basin and its margins. Pini et al. (2012) note that a retrogressive failure may cut back to the basin margin and successively mix shallow marine sediments with nearshore and onshore sediments. Thus, the presence of onshore material in such deposits does not necessarily demand tsunami-related coastal flooding and subsequent washing of the material into the sea.

Future research in Hornitos demands geophysical surveys exposing the internal structures of the lowest terrace. Such studies may trace the extent of Unit VI and obtain information on the dimensions of the rock slabs incorporated in the deposit. The combination of geophysical and sedimentological data will help to broaden the picture of event deposition in the Bay of Mejillones.

6. Conclusions

We re-evaluated the origin of a Pliocene coarse-clastic unit contained in the La Portada Formation at Caleta Hornitos in northern Chile, which was previously interpreted as a submarine tsunami backwash deposit by Hartley et al. (2001). The formation of this unit later was attributed to the Eltanin impact and its Pacific-wide tsunami (Felton and Crook, 2003; Goff and Dominey-Howes, 2010; Goff et al., 2012).

Our analysis of the sediment bed (Unit VI) differs from the original description by the fact that the unit represents a coarse clastic megabreccia containing large rock slabs instead of being referred to as a 'conglomerate bed'. Secondly, Unit VI is intercalated into shallow-marine breccia layers of smaller scale, which represent the similarly high-energetic background sedimentation. The presence of large rock slabs several tens of meters long, implies the emplacement of the unit by a high-density debris flow with possible hydroplaning at its base and front. Soft-sediment deformation and sand dykes underline a debris flow origin. The comparison to recent submarine tsunami sediments shows that there are hardly any similarities, most notably because Unit VI was deposited en masse without any obvious vertical (e.g., grading) or horizontal (e.g., sediment bypassing) trends.

Increased tectonic activity started in coastal northern Chile during the Pliocene and entailed fast coastal uplift and related oversteepening of slopes and coastal cliffs. Cliff or margin collapses, most probably triggered by earthquakes, were frequent during this time and can explain both the background sediments and the occurrence of the megabreccia. Deposition from a retrogressive slide mixing components from both the shallow marine basin and alluvial environments including alluvial fans, beaches, cliffs and local basement rocks is the interpretation most compatible with the available data.

A connection to the Eltanin impact can be excluded because numerical models including the shoaling effect in shelf regions, indicate that, if at all, such an impact did not cause large onshore wave heights at Hornitos and seismic shaking caused by the deep-sea impact probably was not severe enough to trigger submarine mass movements as far as several thousand kilometers from the impact site. Moreover, biostratigraphic ages seem to imply that the La Portada Formation predates the Eltanin impact. Most strikingly, the tectonic background during the deposition of the La Portada Formation and the nature of the likewise high-energetic depositional environment, underline that Unit VI has not been emplaced by tsunami activity of any kind, but instead resembles a mass wasting deposits of different scales.

Acknowledgments

This study was supported by grant BA 1011/32-1 of the German Research Foundation (DFG). I. Krel (Münster) analyzed the matrix composition of several samples from Hornitos during her bachelor thesis. Thanks to H.-G. Wilke (Universidad Católica del Norte, Antofagasta) for helpful discussions on the local geology of the Mejillones Peninsula. We thank A. Switzer and D. Tappin for their constructive reviews, as well as Editor J. Knight for helpful comments.

References

Abbate, E., Bortolotti, V., Passerini, P., 1970. Olistostromes and olistoliths. Sedimentary Geology 4, 521–557.

Arai, K., Naruse, H., Miura, R., Kawamura, K., Hino, R., Ito, Y., Inazu, D., Yokokawa, M., Izumi, N., Murayama, M., Kasaya, T., 2013. Tsunami-generated turbidity current of the 2011 Tohoku-Oki earthquake. Geology 41, 1195–1198.

Bahlburg, H., Spiske, M., 2012. Sedimentology of tsunami inflow and backflow deposits: key differences revealed in a modern example. Sedimentology 59, 1063–1086.

Bahlburg, H., Weiss, R., 2007. Sedimentology of the December 26, 2004, Sumatra tsunami deposits in eastern India (Tamil Nadu) and Kenya. International Journal of Earth Sciences 96, 1195–1209.
Bahlburg, H., Spiske, M., Weiss, R., 2010. Comment on "Sedimentary features of tsunami backwash deposits in a shallow marine Miocene setting, Mejillones Peninsula, northern Chile" by G. Cantalamessa and C. Di Celma [Sedimentary Geology 178 (2005) 259–273]. Sedimentary Geology 228, 77–80.
Bailey, E.B., Weir, J., 1932. Submarine faulting in Kimmeridgian times: east Sutherland. Transactions of the Royal Society of Edinburgh 57, 429–467.
Ballance, P.F., Gregory, M.R., Gibson, G.W., 1981. Coconuts in Miocene turbidites in New Zealand possible evidence for tsunami origin of some turbidity currents. Geology 9, 592–595.
Borrero, J.C., 2005. Field data and satellite imagery of tsunami effects in Banda Aceh. Science 308, 1596.
Boslough, M.E., Chael, E.P., Trucano, T.G., Crawford, D.A., Campbell, D.L., 1996. Axial focusing of impact energy in the Earth's interior: a possible link to flood basalts and hotspots. In: Ryder, G., Fastovsky, D.E., Gartner, S. (Eds.), The Cretaceous–Tertiary Event and Other Catastrophes in Earth History. Geological Society of America Special Paper, 307, pp. 541–550.
Bourgeois, J., 2009. Chapter 3 — Geologic Effects and Records of Tsunamis. In: Robinson, A.R., Bernard, E.N. (Eds.), The Sea 15, Tsunamis. Harvard University Press, Cambridge, pp. 53–91.
Bralower, T.J., Paull, C.K., Leckie, R.M., 1998. The Cretaceous–Tertiary boundary cocktail: Chicxulub impact triggers margin collapse and extensive sedimentary gravity flows. Geology 26, 331–334.
Brookfield, M.E., Blechschmidt, I., Hannigan, R., Coniglio, M., Simonson, B., Wilson, G., 2006. Sedimentology and geochemistry of extensive very coarse deepwater submarine fan sediments in the Middle Jurassic of Oman, emplaced by giant tsunami triggered by submarine mass flows. Sedimentary Geology 192, 75–98.
Camerlenghi, A., Pini, G.A., 2009. Mud volcanoes, olistostromes and Argille scagliose in the Mediterranean region. Sedimentology 56, 319–365.
Cantalamessa, G., Di Celma, C., 2005. Sedimentary features of tsunami backwash deposits in a shallow marine Miocene setting, Mejillones Peninsula, northern Chile. Sedimentary Geology 178, 259–273.
Dawson, A.G., Stewart, I., 2008. Offshore tractive current deposition — the forgotten tsunami sedimentation process. In: Shiki, T., Tsuji, Y., Minoura, K., Yamazaki, T. (Eds.), Tsunamiites. Elsevier, pp. 153–161.
Day, S., Maslin, M., 2005. Linking large impacts, gas hydrates, and carbon isotope excursions through widespread sediment liquefaction and continental slope failure: the example of the K–T boundary event. In: Kenkmann, T., Hörz, F., Deutsch, A. (Eds.), Large Meteorite Impacts III. Geological Society of America Special Paper, 384, pp. 239–258.
Di Geronimo, I., Choowong, M., Phantuwongraj, S., 2009. Geomorphology and superficial bottom sediments of Khao Lak coastal area (SW Thailand). Polish Journal of Environmental Studies 18, 111–121.
Encinas, A., Le Roux, J.P., Buatois, L.A., Nielsen, S.N., Finger, K.L., Fourtanier, E., Lavenu, A., 2006. Nuevo esquema estratigráfico para los depósitos Mio-Pliocenos del área de Navidad (33°00′–34°30′S), Chile central. Revista Geologica de Chile 33, 221–246.
Feldens, P., Schwarzer, K., Szczucinski, W., Stattegger, K., Sakuna, D., Somgpongchaiykul, P., 2009. Impact of 2004 tsunami on seafloor morphology and offshore sediments, Pakarang Cape, Thailand. Polish Journal of Environmental Studies 18, 63–68.
Feldens, P., Schwarzer, K., Sakuna, D., Szczucinski, W., Somgpongchaiykul, A., 2012. Sediment distribution on the inner continental shelf off Khao Lak (Thailand) after the 2004 Indian Ocean tsunami. Earth, Planets and Space 64, 875–887.
Felton, E.A., Crook, K.A.W., 2003. Evaluating the impacts of huge waves on rocky shorelines: an essay review of the book 'Tsunami — The Underrated Hazard'. Marine Geology 197, 1–12.
Ferraris, F., Di Biase, F., 1978. Hoja Antofagasta. Carta Geológica de Chile, Escala 1:250,000. Instituto de Investigaciones Geológicas, Santiago, No 30, 48 p.
Festa, A., Pini, G.A., Dilek, Y., Codegone, G., 2010. Mélanges and mélange-forming processes: a historical overview and new concepts. International Geology Review 52, 1040–1105.
Finger, K.L., Nielsen, S.N., Devries, T.J., Encinas, A., Peterson, D.E., 2007. Paleontologic evidence for sedimentary displacement in Neogene forearc basins of central Chile. Palaios 22, 3–16.
Flores, G., 1956. The results of the studies on petroleum exploration in Sicily: discussion. Bollettino del Servizio Geologico d'Italia 78, 46–47.
Frederichs, T., Bleil, U., Gersonde, R., Kuhn, G., 2002. Revised age of the Eltanin impact in Southern Ocean. Eos, Transactions American Geophysical Union 83, F794.
Geersen, J., Völker, D., Behrmann, J.H., Reichert, C., Krastel, S., 2011. Pleistocene giant slope failures offshore Arauco Peninsula, southern Chile. Journal of the Geological Society 168, 1237–1248.
Gersonde, R., Kyte, F.T., Bleil, U., Diekmann, B., Flores, J.A., Gohl, K., Grahl, G., Hagen, R., Kuhn, G., Sierro, F.J., Volker, D., Abelmann, A., Bostwick, J.A., 1997. Geological record and reconstruction of the late Pliocene impact of the Eltanin asteroid in the Southern Ocean. Nature 390, 357–363.
Gisler, G.R., Weaver, R.P., Mader, C.L., Gittings, M.L., 2004. Two- and three-dimensional asteroid impact simulations. Computing in Science and Engineering 6, 46–55.
Gisler, G.R., Weaver, R.P., Gittings, M.L., 2011. Calculations of asteroid impacts into deep and shallow water. Pure and Applied Geophysics 168, 1187–1198.
Goff, J., Dominey-Howes, D., 2010. Does the Eltanin asteroid tsunami provide an alternative explanation for the Australian megatsunami hypothesis? Natural Hazards and Earth Systems Science 10, 713–715.
Goff, J., Chagué-Goff, C., Archer, M., Dominey-Howes, D., Turney, C., 2012. The Eltanin asteroid impact: possible South Pacific palaeomegatsunami footprint and potential implications for the Pliocene–Pleistocene transition. Journal of Quaternary Science 27, 660–670.
González, J., Carrizo, D., Macci, A., Schneider, H., 2003. The link between forearc tectonics and Pliocene–Quaternary deformation of the Coastal Cordillera, northern Chile. Journal of South American Earth Sciences 16, 321–342.
Google Earth, 2010. Bay of Mejillones, Chile. 22° 54' 16.79"S, 70° 16' 18.87"W, eye altitude 1.32 km, image date 18. DigitalGlobe http://www.earth.google.com [accessed 04. Oktober 2013].
Goto, K., Tada, R., Tajika, E., Iturralde-Vinent, M.A., Matsui, T., Yamamoto, S., Nakano, Y., Oji, T., Kiyokawa, S., García Delgado, D.E., Díaz Otero, C., Rojas Consuegra, R., 2008. Lateral lithological and compositional variations of the Cretaceous/Tertiary deep-sea tsunami deposits in northwestern Cuba. Cretaceous Research 29, 217–236.
Goto, K., Sugawara, D., Ikema, S., Miyagi, T., 2012. Sedimentary processes associated with sand and boulder deposits formed by the 2011 Tohoku-oki tsunami at Sabusawa Island, Japan. Sedimentary Geology 282, 188–198.
Haraguchi, T., Goto, K., Sato, M., Yoshinaga, Y., Yamaguchi, N., Takahashi, T., 2013. Large bedform generated by the 2011 Tohoku-oki tsunami at Kesennuma Bay, Japan. Marine Geology 335, 200–205.
Hartley, A.J., Jolley, E.J., 1995. Tectonic implications of Late Cenozoic sedimentation from the Coastal Cordillera of northern Chile (22–24°S). Journal of the Geological Society of London 152, 51–63.
Hartley, A., Howell, J., Mather, A.E., Chong, G., 2001. A possible Plio-Pleistocene tsunami deposit, Hornitos, northern Chile. Revista Geologica de Chile 28, 117–125.
Hassler, S.W., Robey, H.F., Simonson, B.M., 2000. Bedforms produced by impact-generated tsunami, 2.6 Ga Hamersley basin, Western Australia. Sedimentary Geology 135, 283–294.
Heezen, B.C., Ewing, M., 1952. Turbidity currents and submarine slumps, and the 1929 Grand Banks earthquake. American Journal of Science 250, 849–873.
Herm, D., 1969. Marines Pliozän und Pleistozän in Nord und Mittel-Chile unter besonderer Berücksichtigung der Entwicklung der Mollusken-Faunen. Zitteliana 2, 1–159.
Hooper, A., Pietrzak, J., Simons, W., Cui, H., Riva, R., Naeije, M., Terwisscha van Scheltinga, A., Schrama, E., Stelling, G., Socquet, A., 2013. Importance of horizontal seafloor motion on tsunami height for the 2011 Mw = 9.0 Tohoku-Oki earthquake. Earth and Planetary Science Letters 361, 469–479.
Huntington, K., Bourgeois, J., Gelfenbaum, G., Lynett, P., Jaffe, B., Yeh, H., Weiss, R., 2007. Sandy signs of a tsunami's onshore depth and speed. Eos, Transactions American Geophysical Union 88, 577–578.
Kawagucci, S., Yukari, T., Yoshida, Y.T., Noguchi, T., Honda, M.C., Uchida, H., Ishibashi, H., Nakagawa, F., Tsunogai, U., Okamura, K., Takaki, Y., Nunoura, T., Miyazaki, J., Hirai, M., Lin, W., Kitazato, H., Takai, K., 2012. Disturbance of deep-sea environments induced by the M9.0 Tohoku earthquake. Nature Scientific Reports 2, 270.
Kiyokawa, S., Tada, R., Iturralde-Vinent, M.A., Tajika, E., Yamamoto, S., Oji, T., Nakano, Y., Goto, K., Takayama, H., Garcia-Delgado, D., Diaz-Otero, C., Rojas-Consuegra, R., Matsui, T., 2002. Cretaceous–Tertiary boundary sequence in the Cacarajicara Formation, western Cuba. In: Koeberl, C., MacLeod, K.G. (Eds.), Catastrophic Events and Mass Extinctions: Impacts and Beyond. Geological Society of America Special Paper, 356, pp. 125–144.
Klaus, A., Norris, R.D., Kroon, D., Smit, J., 2000. Impact-induced K–T boundary mass wasting across the Blake Nose, western North Atlantic. Geology 28, 319–322.
Korycansky, D.G., Lynett, P.J., 2005. Offshore breaking of impact tsunami: the Van Dorn effect revisited. Geophysical Research Letters 32, L10608. http://dx.doi.org/10.1029/2004GL021918.
Kramer, W., Siebel, W., Romer, R.L., Haase, G., Zimmer, M., Ehrlichmann, R., 2005. Geochemical and isotopic characteristics and evolution of the Jurassic volcanic arc between Arica (18°30′S) and Tocopilla (22°S), North Chilean Coastal Cordillera. Chemie der Erde — Geochemistry 65, 47–78.
Kyte, F.T., Brownlee, D.E., 1985. Unmelted meteoritic debris in the Late Pliocene iridium anomaly: evidence for the ocean impact of a nonchondritic asteroid. Geochimica Cosmochimica Acta 49, 1095–1108.
Kyte, F.T., Zhou, Z., Wasson, J.T., 1981. High noble metal concentrations in a late Pliocene sediment. Nature 292, 417–420.
Lavigne, F., Paris, R., Grancher, D., Wassmer, P., Brunstein, D., Vautier, F., Leone, F., Flohic, F., de Coster, B., Gunawan, T., Gomez, C., Setiawan, A., Cahyadi, R., Fachrizal, 2009. Reconstruction of tsunami inland propagation on December 26, 2004 in Banda Aceh, Indonesia, through field investigations. Pure and Applied Geophysics 166, 259–281.
Le Roux, J.P., Elgueta, S., 2000. Sedimentologic development of a Late Oligocene - Miocene forearc embayment, Valdivia Basin Complex, southern Chile. Sedimentary Geology 130, 27–44.
Le Roux, J.P., Vargas, G., 2005. Hydraulic behavior of tsunami backflows: insights from their modern and ancient deposits. Environmental Geology 49, 65–75.
Le Roux, J.P., Gómez, C., Fenner, J., Middleton, H., 2004. Sedimentological processes in a scarp-controlled rocky shoreline to upper continental slope environment, as revealed by unusual sedimentary features in the Neogene Coquimbo Formation, north-central Chile. Sedimentary Geology 165, 67–92.
Le Roux, J.P., Olivares, D.M., Nielsen, S.N., Smith, N.D., Middleton, H., Fenner, J., Ishman, S.E., 2006. Bay sedimentation as controlled by regional crustal behaviour, local tectonics and eustatic sea-level changes: Coquimbo Formation (Miocene–Pliocene), Bay of Tongoy, central Chile. Sedimentary Geology 184, 133–153.
Le Roux, J.P., Nielsen, S.N., Kemnitz, H., Henriquez, Á., 2008. A Pliocene mega-tsunami deposit and associated features in the Ranquil Formation, southern Chile. Sedimentary Geology 203, 164–180.
Liu, P.L.F., Lynett, P., Fernando, H., Jaffe, B.E., Fritz, H., Higman, B., Morton, R., Goff, J., Synolakis, C., 2005. Observations by the International Tsunami Survey Team in Sri Lanka. Science 308, 1595.
Lo Iacono, C., Gràcia, E., Zaniboni, F., Pagnoni, G., Tinti, S., Bartolomé, R., Masson, D.G., Wynn, R.B., Lourenço, N., Pinto de Abreu, M., José Dañobeitia, J., Zitellini, N., 2012.

Large, deepwater slope failures: implications for landslide-generated tsunamis. Geology 40, 931–934.
Locat, J., Lee, H.J., Locat, P., Imran, J., 2004. Numerical analysis of the mobility of the Palos Verdes debris avalanche, California, and its implication for the generation of tsunamis. Marine Geology 203, 269–280.
Mader, C.L., 1998. Modeling the Eltanin asteroid tsunami. Science of Tsunami Hazard 16, 17–21.
Maltman, A., 1994. Introduction and overview. In: Maltman, A. (Ed.), The Geological Deformation of Sediments. Chapman & Hall, London, pp. 1–35.
Martinez, E., Niemeyer, H., 1982. Depósitos marinos aterrazados del Pliocene superior en la ciudad de Antofagasta, su relación con la Falla Atacama. Actas del III Congreso Geoldgico Chileno, 1, pp. Al76–Al88.
Marquardt, C., Lavenu, A., Ortlieb, L., Godoy, E., Comte, D., 2004. Coastal neotectonics in Southern Central Andes: uplift anddeformation of marine terraces in Northern Chile (278S). Tectonophysics 394, 193–219.
Massari, F., D'Alessandro, A., 2000. Tsunami-related scour-and-drape undulations in Middle Pliocene restricted-bay carbonate deposits (Salento, south Italy). Sedimentary Geology 135, 265–281.
Masson, D., Harbitz, C.B., Wynn, R., Pedersen, G., Lovholt, F., 2006. Submarine landslides: processes, triggers and hazard prediction. Philosophical Transactions of the Royal Society A: Mathematical, Physical and Engineering Sciences 364, 2009–2039.
Mather, A.E., Hartley, A.J., Griffiths, J.S., 2014. The giant coastal landslides of Northern Chile: tectonic and climatic interactions on a classic convergent plate margin. Earth and Planetary Science Letters 388, 249–256.
Melosh, H.J., 2003. Impact-generated tsunamis: an overrated hazard. Proceedings of the Lunar Planetary Science Conference (http://www.lpi.usra.edu/meetings/lpsc2003/pdf/2013.pdf).
Michalík, J., 1997. Tsunamites in a storm-dominated Anisian carbonate ramp (Vysoká Formation; Malé Karpaty Mts., Western Carpathians). Geologica Carpathica 48, 221–229.
Mohrig, D., Ellis, C., Parker, G., Whipple, K.X., Hondzo, M., 1998. Hydroplaning of subaqueous debris flows. Geological Society of America Bulletin 110, 387–394.
Mulder, T., Alexander, J., 2001. The physical character of subaqueous sedimentary density flows and their deposits. Sedimentology 48, 269–299.
Mulder, T., Cochonat, P., 1996. Classification of offshore mass movements. Journal of Sedimentary Research 66, 43–57.
Murty, T.S., 1982. Comment on 'Coconuts in Miocene turbidites in New Zealand: possible evidence for tsunami origin of some turbidity currents'. Geology 10, 489.
Niemeyer, H., González, G., Martinez, E., 1996. Evolución tectónica cenozoica del margen continental activo de Antofagasta, norte de Chile. Revista Geologica de Chile 23, 165–186.
Noda, A., Katayama, H., Sagayama, T., Suga, K., Uchida, Y., Satake, K., Abe, K., Okamura, Y., 2007. Evaluation of tsunami impacts on shallow marine sediments: an example from the tsunami caused by the 2003 Tokachi-oki earthquake, northern Japan. Sedimentary Geology 200, 314–327.
Norris, R.D., Firth, J., Blusztajn, J.S., Ravizza, G., 2000. Mass failure of the North Atlantic margin triggered by the Cretaceous–Paleogene bolide impact. Geology 28, 1119–1122.
Ortlieb, L., Zazo, C., Goy, J., Hillaire-Marcel, C., Ghaleb, B., Cournoyer, L., 1996. Coastal deformation and sea-level changes in the northern Chile subduction area (238°S) during the last 330 ky. Quaternary Science Reviews 15, 819–831.
Pardo-Casas, F., Molnar, P., 1987. Relative motion of the Nazca (Farallon) and South American Plates since late Cretaceous time. Tectonics 6, 233–248.
Paris, R., Fournier, J., Poizot, E., Etienne, S., Morin, J., Lavigne, F., Wassmer, P., 2010. Boulder and fine sediment transport and deposition by the 2004 tsunami in Lhok Nga (western Banda Aceh, Sumatra, Indonesia): a coupled offshore–onshore model. Marine Geology 268, 43–54.
Parsons, J.D., Friedrichs, C.T., Traykovski, P.A., Mohrig, D., Imran, J., Syvitski, J.P.M., Parker, G., Puig, P., Buttles, J.L., García, M.H., 2007. The mechanics of marine sediment gravity flows. In: Nittrouer, C., Austin, J., Field, M., Kravitz, J., Syvitski, J., Wiberg, P. (Eds.), Continental Margin Sedimentation — From Sediment Transport to Sequence Stratigraphy. International Association of Sedimentologists Special Publications, 37, pp. 275–337.
Paskoff, R., 1989. Zonality and main geomorphic features of the Chilean coast. Essener Geographische Arbeiten 18, 237–267.
Pichowiak, S., Buchelt, M., Damm, K.-W., 1990. Magmatic activity and tectonic setting of the early stages of the Andean cycle in northern Chile. In: Kay, S.M., Rapela, C.W. (Eds.), Plutonism from Antarctica to Alaska. Geological Society of America Special Paper, 241, pp. 101–126.
Pickering, K.T., 1984. The Upper Jurassic "boulder beds" and related deposits; a fault-controlled submarine slope, NE Scotland. Journal of the Geological Society of London 141, 357–374.
Pini, G.A., Ogata, K., Camerlenghi, A., Festa, A., Lucente, C.C., Codegone, G., 2012. Sedimentary mélanges and fossil mass-transport complexes: a key for better understanding submarine mass movements. In: Yamada, Y., Kawamura, K., Ikehara, K., Ogawa, Y., Urgeles, R., Mosher, D., Chaytor, J., Strasser, M. (Eds.), Submarine Mass Movements and their Consequences: Advances in Natural and Technological Hazards Research, 31. Springer, pp. 585–594.
Powell, J.A., Ishman, S.E., Wilke, H.G., 2005a. Foraminifera from the Cerro Bandurria and Hornitos sections, Mejillones Peninsula, northern Chile. MEEC 2005, Paleoecology Symposium (http://mypage.siu.edu/meec2005/Abs_PaleoEcol.html).
Powell, J.A., Ishman, S.E., Hartley, A.J., Mather, A., Wilke, H.G., 2005b. Age and paleoenvironmental interpretations of foraminiferal data from the Hornitos locality, northern Chile. Eos, Transactions of the American Geophysical Union 86 (Abstract PP23B-02).
Pratt, B.R., 2001. Oceanography, bathymetry and syndepositional tectonics of a Precambrian intracratonic basin: integrating sediments, storms, earthquakes and tsunamis in the Belt Supergroup (Helena Formation, ca. 1.45 Ga), western North America. Sedimentary Geology 141–142, 371–394.
Pratt, B.R., 2002. Storms versus tsunamis: dynamic interplay of sedimentary, diagenetic, and tectonic processes in the Cambrian of Montana. Geology 30, 423–426.
Richmond, B.M., Jaffe, B.E., Gelfenbaum, G., Morton, R.A., 2006. Geologic impacts of the 2004 Indian Ocean tsunami on Indonesia, Sri Lanka, and the Maldives. Zeitschift für Geomorphologie Supplement Issues 146, 235–251.
Richmond, B., Szczuciński, W., Chagué-Goff, C., Goto, K., Sugawara, D., Witter, R., Tappin, D.R., Jaffe, B.E., Fujino, S., Nishimura, Y., Goff, J., 2012. Erosion, deposition and landscape change on the Sendai coastal plain, Japan, resulting from the March 11, 2011 Tohoku-oki tsunami. Sedimentary Geology 282, 27–39.
Rossetti, D.D.F., Goes, A.M., Truckenbrodt, W., Anaisse Jr., J., 2000. Tsunami-induced large-scale scour-and-fill structures in Late Albian to Cenomanian deposits of the Grajau Basin, northern Brazil. Sedimentology 47, 309–323.
Sarkar, S., Bose, P.K., Eriksson, P.G., 2011. Neoproterozoic tsunamiite: Upper Bhander Sandstone, Central India. Sedimentary Geology 238, 181–190.
Scasso, R.A., Concheyro, A., Kiessling, W., Aberhan, M., Hecht, L., Medina, F.A., Tagle, R., 2005. A tsunami deposit at the Cretaceous/Paleogene boundary in the Neuquén Basin of Argentina. Cretaceous Research 26, 283–297.
Schnyder, J., Baudin, F., Deconinck, J.F., 2005. A possible tsunami deposit around the Jurassic–Cretaceous boundary in the Boulonnais area (northern France). Sedimentary Geology 177, 209–227.
Shanmugam, G., 2012. Process-sedimentological challenges in distinguishing paleotsunami deposits. Natural Hazards 63, 5–30.
Shiki, T., 1996. Reading of the trigger records of sedimentary events — a problem for future studies. Sedimentary Geology 104, 249–255.
Shiki, T., Tachibana, T., 2008. Sedimentology of tsunamiites reflecting chaotic events in the geological record — significance and problems. In: Shiki, T., Tsuji, Y., Minoura, K., Yamazaki, T. (Eds.), Tsunamiites. Elsevier, pp. 341–358.
Shiki, T., Yamazaki, T., 1996. Tsunami-induced conglomerates in Miocene upper bathyal deposits, Chita Peninsula, central Japan. Sedimentary Geology 104, 175–188.
Shiki, T., Tachibana, T., Fujiwara, O., Goto, K., Nanayama, F., Yamazaki, T., 2008. Characteristic features of tsunamiites. In: Shiki, T., Tsuji, Y., Minoura, K., Yamazaki, T. (Eds.), Tsunamiites. Elsevier, pp. 319–337.
Shuvalov, V.V., Trubetskaya, I.A., 2007. Numerical modeling of the formation of the Eltanin submarine impact structure. Solar System Research 41, 56–64.
Spiske, M., Piepenbreier, J., Benavente, C., Bahlburg, H., 2013. Preservation potential of tsunami deposits on arid siliciclastic coasts. Earth-Science Reviews 126, 58–73.
Strasser, M., Hilbe, M., Anselmetti, F.S., 2011. Mapping basin-wide subaquatic slope failure susceptibility as a tool to assess regional seismic and tsunami hazards. Marine Geophysical Research 32, 331–347.
Suárez, G., Comte, D., 1993. Comment on "Seismic coupling along Chilean subduction zone" by B.W. Tichelaar, L.R. Ruff. Journal of Geophysical Research 98, 15825–15828.
Sugawara, D., Minoura, K., Imamura, F., 2008. Tsunamis and tsunami sedimentology. In: Shiki, T., Tsuji, Y., Minoura, K., Yamazaki, T. (Eds.), Tsunamiites. Elsevier, pp. 9–51.
Switzer, A.D., Srinivasalu, S., Thangadurai, N., Ram Mohan, V., 2012. Bedding structures in Indian tsunami deposits that provide clues to the dynamics of tsunami inundation. In: Terry, J.P., Goff, J. (Eds.), Natural Hazards in the Asia–Pacific Region. Geological Society London, Special Publications, 361, pp. 61–77.
Tachibana, T., 2013. Lonestones as indicators of tsunami deposits in deep-sea sedimentary rocks of the Miocene Morozaki Group, central Japan. Sedimentary Geology 289, 62–73.
Talling, P.J., Masson, D.G., Sumner, E.J., Malgenini, G., 2012. Subaqueous sediment density flows: depositional processes and deposit types. Sedimentology 59, 1937–2003.
Tappin, D.R., 2012. Mass transport events and their tsunami hazard. In: Yamada, Y., Kawamura, K., Ikehara, K., Ogawa, Y., Urgeles, R., Mosher, D., Chaytor, J., Strasser, M. (Eds.), Submarine Mass Movements and their Consequences: Advances in Natural and Technological Hazards Research, 31. Springer, pp. 667–684.
Tappin, D.R., Matsumoto, T., Watts, P., Satake, K., MCMurtry, G.M., Matsuyama, Y., Lafoy, Y., Tsuji, Y., Kanamatsu, T., Lus, W., Iwabuchi, Y., Yeh, H., Matsumotu, Y., Nakamura, M., Mahoi, M., Hill, P., Crook, K., Anton, L., Walsh, J.P., 1999. Sediment slump likely caused 1998 Papua New Guinea tsunami. EOS. Transactions of the American Geophysical Union 80 (329, 334, 340).
Vargas, G., Ortlieb, L., Chapron, E., Valdes, J., Marquardt, C., 2005. Paleoseismic inferences from a high-resolution marine sedimentary record in northern Chile (23°S). Tectonophysics 399, 381–398.
Victor, P., Sobiesak, M., Glodny, J., Nielsen, S.N., Oncken, O., 2011. Long-term persistence of subduction earthquake segment boundaries: evidence from Mejillones Peninsula, northern Chile. Journal of Geophysical Research 116, B02402. http://dx.doi.org/10.1029/2010JB007771.
Völker, D., Weinrebe, R.W., Behrmann, J.H., Bialas, J., Klaeschen, D., 2009. Mass wasting at the base of the South central Chilean continental margin: the Reloca Slide. Advances in Geosciences 22, 155–167.
Walsh, S.A., Martill, D.M., 2006. A possible earthquake-triggered mega-boulder slide in a Chilean Mio-Pliocene marine sequence: evidence for rapid uplift and bonebed genesis. Journal of the Geological Society 163, 697–705.
Ward, S., Asphaug, E., 2002. Impact tsunami — Eltanin. Deep-Sea Research II 49, 1073–1079.
Weiss, R., Bahlburg, H., 2006. A note on the preservation potential of offshore tsunami deposits. Journal of Sedimentary Research 76, 1267–1273.
Weiss, R., Wünnemann, K., Bahlburg, H., 2006. Numerical modelling of generation, propagation and run-up of tsunamis caused by oceanic impacts: model strategy and technical solutions. Geophysical Journal International 167, 77–88.
Wünnemann, K., Weiss, R., Hofmann, K., 2007. Characteristics of oceanic impact-induced large water waves — re-evaluation of the tsunami hazard. Meteoritics and Planetary Science 42, 1893–1903.

Wünnemann, K., Collins, G.S., Weiss, R., 2010. Impact of a cosmic body into earth's ocean and the generation of large tsunami waves: insight from numerical modeling. Reviews of Geophysics 48, RG4006. http://dx.doi.org/10.1029/2009RG000308.

Wünnemann, K., Elbeshausen, D., Weiss, R., 2011. Comparison of tsunami waves generated by meteorite impacts and landslides. Abstract No. 20–7 Proceedings of Fragile Earth: Geological Processes from Global to Local Scales and Associated Hazards, 4–7 September, Munich, Germany (https://gsa.confex.com/gsa/2011FE/finalprogram/abstract_189678.htm).